RETINAL IMAGE QUALITY IN THE HUMAN EYE AS A FUNCTION OF THE ACCOMMODATION

Norberto López-Gil, Ignacio Iglesias and Pablo Artal

Laboratorio de Optica, Departamento de Física,
Universidad de Murcia,
Campus de Espinardo (Edificio C),
30071 Murcia, Spain.
(http://lo.um.es)

Vision Research
Volume : 38
Issue : 19
Date : 03-Jul-1998

Key words: optical transfer function, accommodation, aberrations, human eye

The changes in the retinal image quality with accommodation in the human eye were studied by using a near-infrared double-pass apparatus. A slightly better modulation transfer function (MTF) in the unaccommodated eye with respect to the accommodated eye was found when using an artificial pupil with a fixed diameter. The technique allows to estimate the MTF of the accommodated eye discounting the effect of the accommodative defocus error. Most of the reduction found in the MTF with accommodation could be explained in terms of the accommodative defocusing error. However, the shape of the retinal images clearly changes with accommodation indicating that other aberrations are also altered with accommodation. In general, the double-pass image for the accommodated eye tends to be more symmetric than the corresponding to the unaccommodated eye. This is probably due either to a decrease in the amount of coma-like aberrations with accommodation or to an increase of other symmetric aberrations, such as defocus or spherical aberration, that hide the asymmetries present in the retinal image of the unaccommodated eye.

INTRODUCTION

How the retinal image quality changes as a function of accommodation is a non completely solved question in Physiological Optics with important implications. For instance, recent studies show that the image quality may play a role in the emmetropization processes (Bartmann and Schaeffel, 1994), and the post-development refractive state could be influenced by the accommodative mechanism (Wildsoet, Howland, Falconer and Dick, 1993). Furthermore, the changes in ocular aberrations with accommodation could serve as optical cues during the accommodation process (Kruger, Mathews, Katz, Aggarwala and Nowbotsing, 1997).

Most previous studies of retinal image quality have been carried out either under cycloplegia (with the accommodation paralyzed) or under natural viewing with a stimulus placed at a fixed distance (Arnulf, 1965; Berny and Slansky, 1969; Howland and Howland, 1976; Walsh, Charman and Howland, 1984; Santamaría, Artal and Bescós, 1987; Liang, Grimm, Goelz and Bille, 1994; Artal, Iglesias, López-Gil and Green, 1995). However, since the eye undergoes substantial optical changes during accommodation, ocular aberrations could change from one accommodative state to another, modifying the associated retinal image quality. The different amount of defocus in the eye for a particular object vergence, or accommodative error, has been studied for different conditions by a large number of researchers (see Ciuffreda, 1991, for a review). Other than defocus, the most studied monochromatic aberration as a function of accommodation has been spherical aberration (Berny and Slansky, 1969; Ivanoff, 1947; Jenkins, 1963; Koomen, Tousey and Scolnik, 1949). These authors suggested that the amount of spherical aberration decreases with accommodation, although most of those results were subject-dependent. Glasser and Campbell (1998) showed in young isolated human lenses that the spherical aberration tends to become more negative with accommodation. Moreover, some results showed clear differences in two perpendicular meridians of the same eye and even asymmetries in the same meridian (Jenkins, 1963). These results cannot be interpreted as a measurement of only a rotational symmetric aberration, as is the spherical aberration, rather they indicate that these spherical aberration measurements also included other asymmetric aberrations. This fact is in agreement with the results of several authors, that by using different techniques, found important contributions of coma-like aberrations even in the fovea (Smirnov, 1961; Howland and Howland, 1977; Liang, *et al.*, 1994; Artal *et al.*, 1995a).

Only a few research groups have addressed the problem of how other aberrations change with accommodation. Howland and Buettner (1989) calculated the changes in the Taylor coefficient of the wave aberration after analyzing van den Brink's defocus maps for

different positions in the pupil (van den Brink, 1962). Lu, Munger and Campbell, (1993) used a vernier method (Campbell, Harrison and Simonet, 1990) to measure the changes in those coefficients in only one meridian. Atchison, Collins and collaborators (Atchison, Collins, Wildsoet, Christensen, and Waterworth, 1995; Collins, Wildsoet, and Atchison, 1995) studied the changes in the wave aberration with accommodation by using an objective version (Walsh *et al.*, 1984) of the cross-cylinder aberroscope (Howland and Howland, 1977). The results of these studies show a change in the coefficients of the aberration with accommodation, although it is strongly dependent on the observer. However, there is not a clear tendency of any of the aberration coefficients related with accommodation, except for the third order spherical aberration that, in general, seems to decrease with accommodation.

In this paper, we explore how the retinal image quality changes with accommodation. We use the double-pass method (Santamaría *et al.*, 1987) to estimate the optical performance of both the accommodated and unaccommodated eye. The double-pass method has been applied in several studies to measure the optical performance in eyes with paralyzed accommodation (Artal and Navarro, 1994; Williams, Artal, Navarro, McMahon and Brainard, 1996). However, in this particular study where normal viewing conditions were required, its application was limited by the fact that the visible point source used in the double-pass measurements was so bright that it dazzles the subject. As a consequence, it prevents proper accommodation to the stimulus and makes it impossible to correctly measure the eye's optical image quality. This problem can be avoided by using near-infrared light (784 nm) in the double-pass apparatus. For this wavelength, the average luminance efficiency of the human eye is five orders of magnitude lower than for a red visible light of 632.8 nm (Griffin, Hubbard and Wald, 1947; Lamb, 1995). An infrared measuring beam of this wavelength does not affect the accommodation response and allows to estimate the eye's optical performance in visible light (López-Gil and Artal, 1997).

METHODS

Infrared double-pass apparatus

Figure 1 shows the experimental set-up based on the infrared double-pass apparatus described in detail elsewhere (López-Gil and Artal, 1997). In the present study, we modified the first pass so that there are two independent optical paths, one for the stimulus to accommodate (E) and another for the near-infrared point source

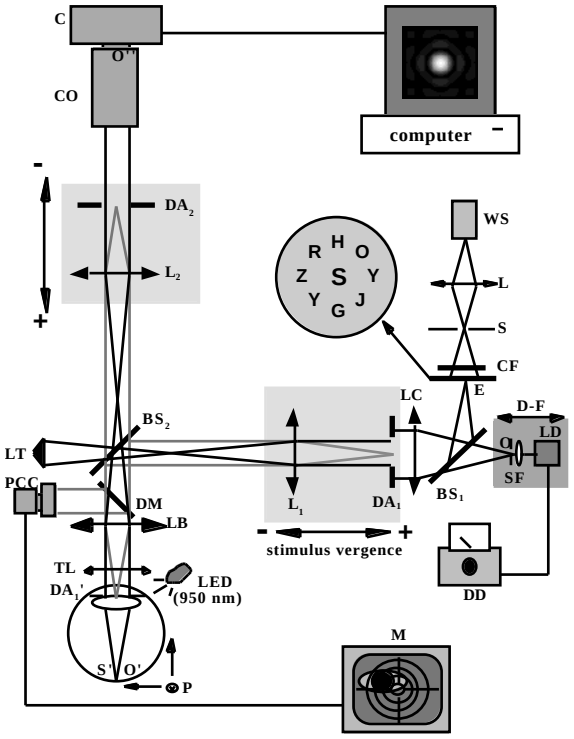

Figure 1.- Experimental set-up. LD, laser diode; DD diode driver; SF spatial filter, BS_1, BS_2, pellicle beam splitters; WS white light source; L, convergence lens; S, small stop; CF, color filter; E, stimulus for accommodation; LC, L_1, LB, and L_2, achromatic doublets; DA_1 and DA_2, first and second pass stop respectively; LT, light trapper; TL, trial lens; P, eye positioner; DM, dichroic mirror; PCC, camera CCD for pupil centering; M, monitor; CO, camera objective; C cooled CCD camera.

(O). This change allows the system to compensate for the difference in focus between O and E caused by the ocular longitudinal chromatic aberration (see below). The system is also designed so that the second pass independently focuses with respect to the first pass; that is, the CCD camera plane is conjugated with a plane in the retina that either can or cannot match the image plane (O') of the point source (O) after the first pass. This design avoids defocus due to an error in accommodation in the second pass. The point source (O) is produced by an infrared diode laser (LD) emitting at 784 nm. The emerging beam from LD is spatially filtered (SF) to produce both a point source and a rotationally symmetric beam. Apertures DA_1 (5 mm in diameter) and DA_2 (5 or 2 mm diameter) have been placed at the first focal plane of lens L_1 and at the second focal plane of lens L_2, respectively. Each aperture moves together with the lens to assure that they are conjugated with the pupil plane for any position of the lenses. The subject's natural pupil diameter was always slightly larger than 5 mm, due to the low-light level conditions in the laboratory, for any vergence of the stimulus used, which means that

these apertures acted as stops for each pass. Lenses LC, L_1, LB and L_2 are all achromatic doublets, each with a focal distance of 190 mm and an anti-reflection coating for the near-infrared light. The camera objective (CO) has a focal length of 400 mm, and the camera (C) is a slow-scan scientific-grade cooled CCD camera (Spectrasource MCD1000) that records images with 16 bits / pixel. The stimulus is a group of high contrast black letters illuminated with red light (see Fig. 1). For a standard observer under photopic conditions, the average wavelength of the stimulus is 624 nm. The procedure to compensate the chromatic difference in focus between the stimulus and the infrared point source is described in detail below. The stimulus is seen at an angle of 2 degrees, and its luminance from the subject pupil plane was 9.5 cd/m^2. A bite-bar is used to position the subject's head. The experimenter centers the subject's pupil with respect to the infrared beam by actuating two millimetric positioners (P). The subject's pupil is monitored by a subsystem consisting of a dichroic mirror (DM), a CCD video camera (PCC), a monitor (M), and an infrared (950 nm) light emitting diode (LED) to illuminate the pupil. The dichroic mirror transmits 62.9% of the 784 nm light reflected from the retina, while also reflecting at 45 degrees 89.5% of the LED 950 nm infrared light. Although most of the light used to illuminate the pupil does not reach the retinal image plane, we turn off this LED during the exposure time to avoid variations in the background of the double-pass images. The images were recorded with 256x256 pixels, each pixel subtending 0.23 minutes of arc of visual field, that corresponds to a resolution in the spatial frequency domain of 1.02 cycles per degree. In practical terms, with the magnification and wavelength used, the double-pass images were correctly sampled for pupils of 5 mm in diameter. The optical performance of the system alone, measured using a plane mirror instead of the eye, is practically diffraction limited for a 5 mm pupil diameter.

To modify the vergence of the object without changing the size of the retinal image, we moved lens L_1 along the optical axis (see Fig. 1). The stimulus vergence (v), expressed in diopters, is related to the position of L_1 (z), expressed in meters, by:

$$v = \frac{-z}{f'_{LB}\, f'_{L_1}} = -27.7\, z \qquad (1)$$

The origin of distances (z=0) has been taken as the position of L_1 which produces zero vergence. Positive values are reached when lens L_1 moves towards LB, z is measured in millimeters and the experimental error was 0.03 D.

We record a series of two double-pass images with an exposure time of five seconds each, assuring that the coherence of the light is broken after the second pass. The images are accepted if there are no blinks, the subject's head does not move and the accommodation shows no apparent change. These conditions can be verified by feedback from the subjects, comparing the two double-pass images and by following possible changes in pupil diameter during the image capture. The latter task can be done during recording even with the LED turned off because part of the near-infrared light coming back from the retina is captured by the video CCD camera (PCC), producing in this case a negative image of the pupil.

The irradiance produced on the cornea by the near-infrared laser during the exposures was always less than 100 nW/cm^2, well below the maximum permissible exposure (ANSI Z136.1;1993).

Correction of the chromatic difference in focus between the stimulus (E) and the near-infrared source (O)

In the first pass, the chromatic difference in focus between the wavelength corresponding to the stimulus and the near-infrared point source should be compensated to have the images of both objects at the same retinal plane. We measured the chromatic difference in focus (c) in each subject by a subjective procedure. The subject was instructed to move lens L_1 towards LC to reduce the stimulus vergence until reaching the closest position to LC at which the stimulus (E) was in best focus. Five measurements were averaged to obtain the best focus position for the stimulus. The same procedure was used to determine the best focus for the near-infrared source (O), which is still slightly visible at safe intensity levels. We found values of the chromatic differences in focus in four subjects ranging between -0.42 D and -0.52 D. The average value was -0.44 D, very close to the -0.43 D obtained using an analytical expression for the longitudinal chromatic aberrations (Thibos, Ye, Zhang, and Bradley, 1992). This chromatic difference in focus is compensated by moving the block D-F (see Fig. 1) away from LC in order to place the infrared source at a vergence of value c from the subject.

We performed paraxial optics calculations of the first pass to verify if once corrected the chromatic difference in focus for a zero vergence, it remains approximately corrected for any other vergence of the stimulus (O). A factor to be

considered is that the chromatic defocus could also change with accommodation (i.e., *c* being a function of *v*). However, the magnitude of this change is not important (Ivanoff, 1947), particularly for small ranges of accommodation and larger wavelengths (Charman and Tucker, 1978), which are the conditions of our study. For instance, in the Gullstrand-Emsley theoretical eye model, the variation in the chromatic difference of focus between 643.8 nm and 780 nm for an object placed at vergences 0 and -3 D, respectively, is around 0.02 D (Bennett and Rabbetts, 1994). By using this value in our paraxial calculations the modification of the chromatic aberration for the two extremes vergences used was less than a quarter of the experimental error. For simplicity, we did not correct this small error. Moreover, considering the small variability in the values of the chromatic differences among subjects, the distance |O-LC| to correct the chromatic difference in focus was set 20.65 cm for all the subjects.

In the second pass, infrared rays leaving the lens L_2 should arrive collimated at the camera objective to record the images in perfect focus. This means that, in the absence of an accommodative error, the distances from LB to L_1 and from LB to L_2 cannot be the same, but are related by:

$$|LB\text{-}L_2| = |L_1\text{-}LB| + 3.61*c \qquad (2)$$

where the distances are measured in centimeters, *c* is the chromatic difference in focus expressed in diopters and the value 3.61 is the opposite of 27.7 (see Eq. (1)) multiplied by 100 to be expressed in m*cm. We tested equation (2) using a mirror instead of an eye and we found a linear coefficient regression of 0.99994. For simplicity, we will refer to the system as *symmetric* when the distances between L_1, LB and L_2 satisfy equation (2); otherwise the system will be referred to as *asymmetric*.

Subjects

Four trained subjects with ages ranging between 18 and 34 years old participated in this study. They had normal vision without any known ocular pathology or accommodative anomalies and all of them were myopic. We used trial lenses to correct the spherical refraction of each subject, specifically: -2.5 D for subject AM and MC, -4 D for NL and -2 D for PA. To achieve a more accurate refractive correction, every subject moved lens L_1 to find the closest position to lens LC that kept the stimulus in clear focus. This task was carried out under natural viewing conditions. In some of the experiments the accommodation was paralyzed using tropicamide 1%.

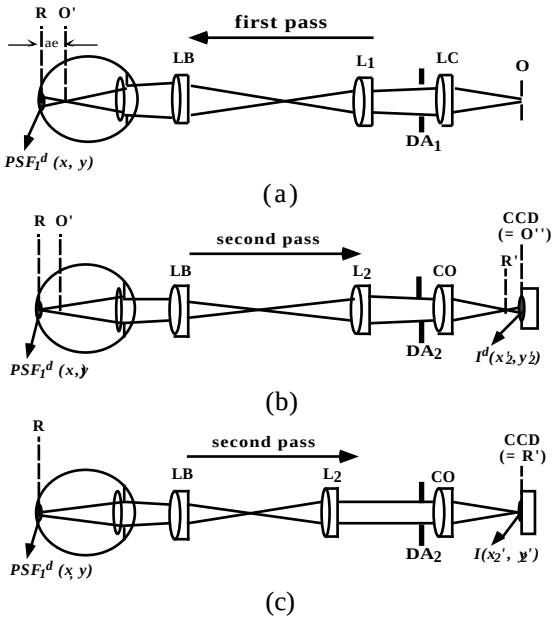

Figure 2.- Schematic diagram of the retinal image formation in the apparatus. (a) In the first pass the near-infrared point source (O) forms an image (O') in the retina (R) in the presence of an accommodative error (ae). (b) This corresponds to a symmetric system in the second pass. R' represents the paraxial image of the retina plane, R, and O'' (conjugated with O') corresponds to the plane of the CCD of the camera. (c) This corresponds to an asymmetric system in the second pass. The lens L_2 is placed to render the retinal plane, R, conjugated with the CCD plane, R'.

Calculation of the modulation transfer function

The double-pass image is the cross-correlation (Artal, Marcos, Navarro and Williams, 1995) between the point spread functions corresponding to the first (PSF_1) and second (PSF_2) passes when both functions are expressed in the same plane, and the position of the exit and entrance pupil match in the first and second pass respectively. Relative to the plane of the retina, with coordinates *x*,*y*, this can be expressed as:

$$I(x'_2, y'_2) = PSF_1(x,y) \quad PSF_2(x,y) \qquad (3)$$

where $I(x'_2, y'_2)$ is the intensity distribution function in the double-pass image and represents a cross-correlation operation (Goodman, 1996). If the eye presents some amount of defocus, for instance due to an accommodative error (ae), as shown schematically in Fig. 2 (a), the double-pass image recorded with a symmetric system is expressed by:

$$I^d(x'_2, y'_2) = PSF_1^d(x,y) \quad PSF_2^d(x,y) \qquad (4)$$

where $PSF_{1,2}^d(x,y)$ are the ocular PSFs, including defocus. Then, the double-pass image can be seen

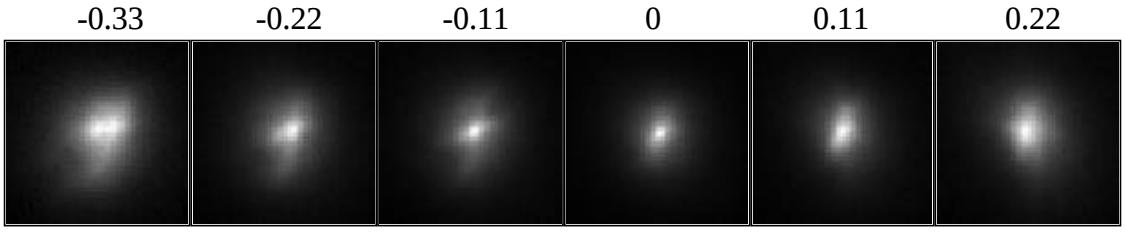

(a)

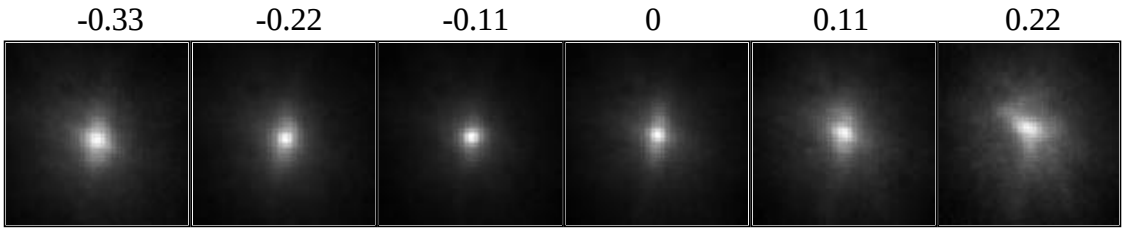

(b)

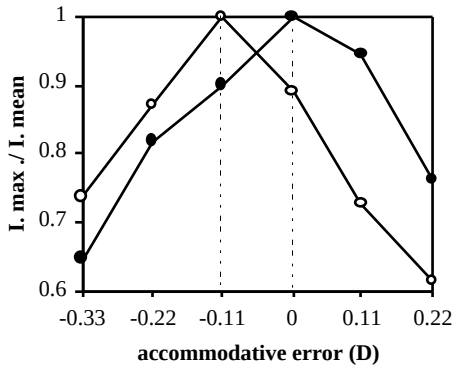

(c)

Figure 3.- Series of double pass images recorded on subject NL when moving lens L_2 in the second pass for an stimulus at the infinite (a) and at 25 cm (b). The number on each image represents the accommodative error in the case that the image were the best of the series. Each image represents an retinal field of 14.7 minutes. c) Maximum irradiance divided by the mean irradiance of each image of the series a) (closed circles) and b) (open circles).

as a blurred image of an already blurred retinal image (see Fig. 2 (b)). The ocular MTF is then calculated taking the square root of the Fourier transform (FT) of the double-pass image (Santamaría *et al.*, 1987):

$$MTF^d(u,v) = \sqrt{\left|FT[I^d(x'_2, y'_2)]\right|} \qquad (5)$$

If, by using a particular asymmetric double-pass set-up, only one of the passes presents defocus, for instance the first pass, equation (3) can be re-written as:

$$I(x'_2, y'_2) = PSF_1^d(x,y) \quad PSF_2(x,y) \qquad (6)$$

where $PSF_2(x,y)$ is the ocular PSF not affected by defocus. The double-pass image corresponds in this case to a correctly focused image of a defocused retinal image (as shown in Fig. 2 (c)). Calculating the Fourier transformation in both terms of equation (6), we have:

$$\left|FT[I(x'_2, y'_2)]\right| = \left|FT[PSF_1^d(x,y)]\right| \left|FT[PSF_2(x,y)]\right| = MTF^d(u,v)\,MTF(u,v) \qquad (7)$$

Equations (5) and (7) are used to calculate the MTF that the eye, with some defocus error in accommodation, would have had if it were in perfect focus:

$$MTF\ (u,v) = \frac{\left|FT[I\ (x'_2, y'_2)]\right|}{\sqrt{\left|FT[I^d(x'_2, y'_2)]\right|}} \qquad (8)$$

In our experimental set-up, the possible defocus of the first pass can be avoided in the second pass by modifying the distance between lenses LB and L_2 until the best double-pass image is found. In that case, the retina and the CCD plane will be conjugated with each other. Figure 3 shows two examples of the method followed to determine the position yielding the best focus image in the case of subject NL. Each image of the series in figures 3 (a) and 3 (b) corresponds to a different position of the lens L_2 in the second pass for a vergence of the stimulus of 0 and -4D, respectively. Figure 3 (c) shows the ratio between the maximum intensity and the average intensity of each image, used as an index of quality to determine the best image in each series.

Experimental procedure

Double-pass images were recorded with three different configurations in the output optical path (second pass) of the apparatus for two stimulus vergences (0 and -4 diopters) in the input optical path (first pass):

a) Equal entrance and exit pupil diameters (5 mm) with symmetric positions of the lenses L_1 and L_2 in both the first and second passes. These double-pass images provide information on the actual image quality of the eye for the stimulus, including any possible accommodative focus error (equation (4)). The MTF is calculated from equation (5).

b) Equal entrance and exit pupil diameters (5 mm) with the position of the lenses in the exit path (L_2) rendering the best double pass image. These double-pass images (equation (6)) provide information on the image quality that the eye should have with a perfect accommodative response (i.e., without accommodative defocus). The MTF corresponding to the best image without focusing error is obtained by equation (8).

c) Unequal entrance and exit pupil diameters (5 and 2 mm) (Artal *et al*., 1995a) with a symmetric set-up in focus. These double-pass images yield the actual shape of the retinal image, including asymmetric aberrations.

RESULTS

Comparison of the eye's MTFs with paralyzed and non-paralyzed accommodation

We first compared the MTFs obtained with and without cycloplegia, under the same experimental conditions, with the stimulus at infinity and a symmetric system for both

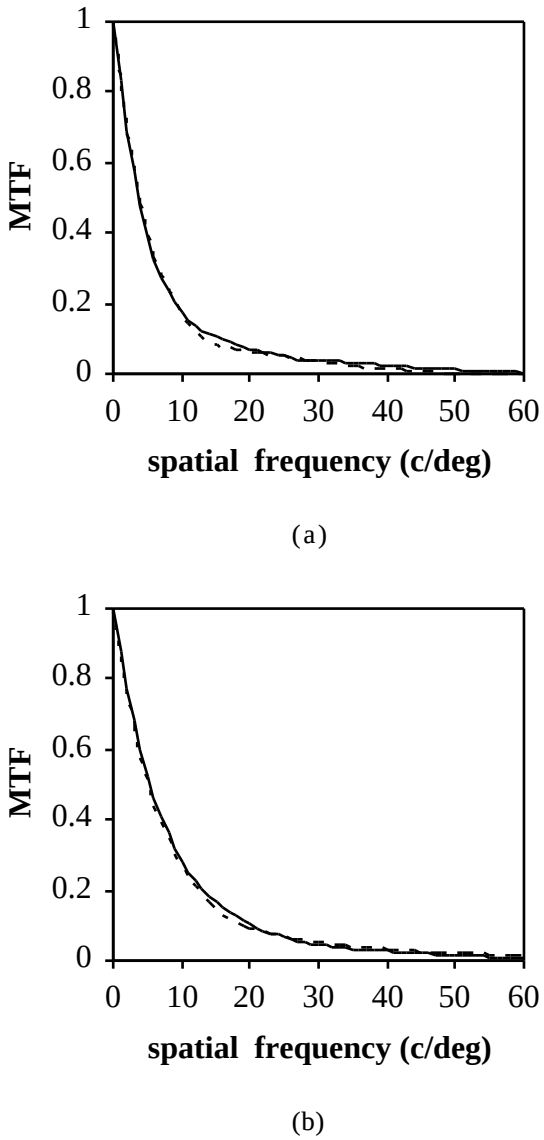

Figure 4.- MTFs (5 mm pupil diameter) for two subjects, AM (a) and NL (b) with a stimulus at infinity. Solid lines represent the MTF obtained with non paralyzed accommodation and dashed lines represent the MTF with paralyzed accommodation.

situations. Since the double-pass images in our experiment were recorded over long exposure, typically five seconds, this comparison is necessary to evaluate the possible effect of the microfluctuations and/or drifts of the accommodation on the MTF results. Figure 4 shows the one-dimensional MTFs obtained in both situations for two subjects. These MTFs were computed by averaging over all directions the two-dimensional MTFs. In the rest of the manuscript, we will refer to these MTFs as the radial profile MTF or simply the MTF. When in the measurements under natural conditions, the accommodation was kept stable during the

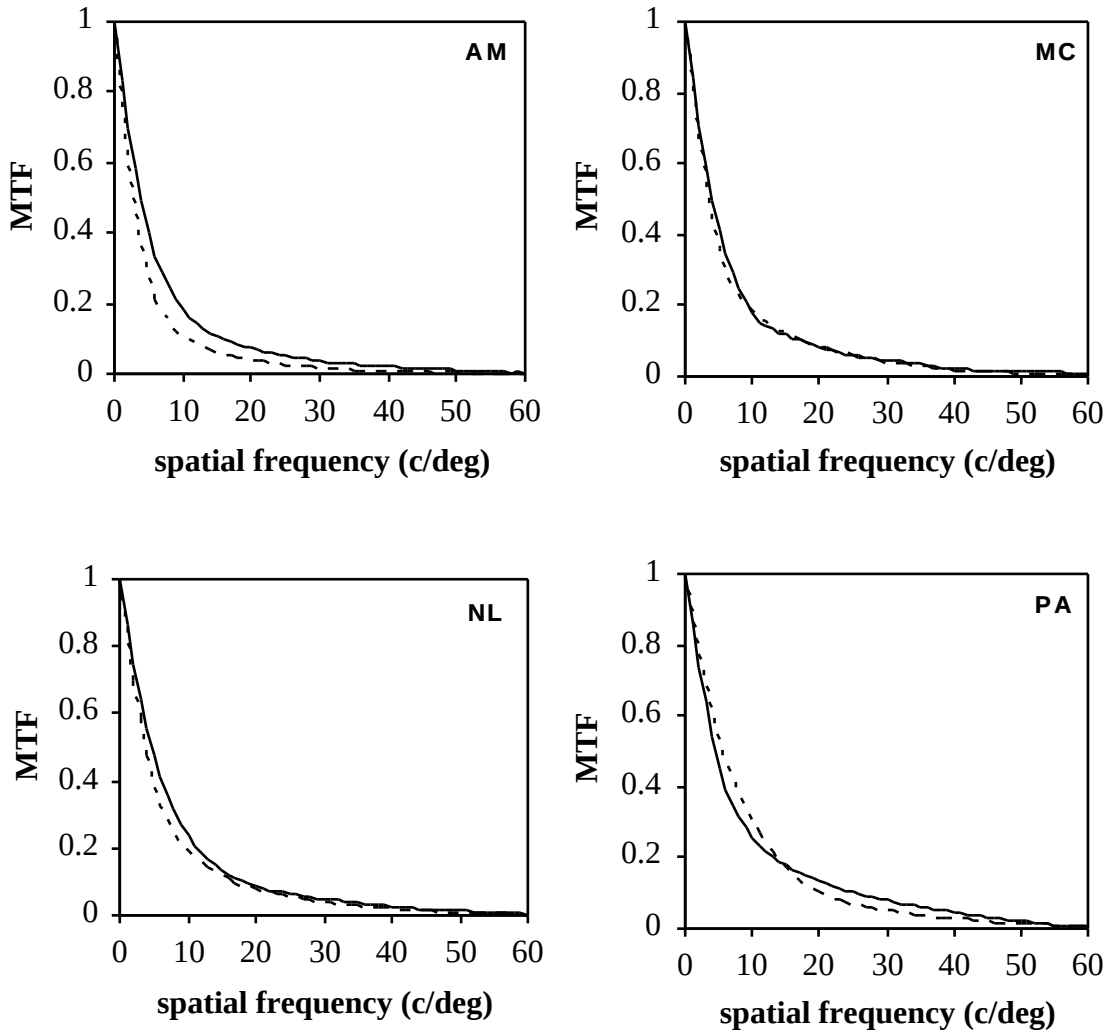

Figure 5.- MTFs (5 mm pupil diameter) of four subjects for a vergence of the stimulus of 0 D and at -4D (-5.5 D for subject MC) in solid and dashed line respectively.

exposure time, the MTFs were very similar to those obtained with paralyzed accommodation. The differences between these MTFs are of the same order than the variability found in MTFs measured under fixed experimental conditions over time. In the following, when comparing MTFs, we will note two MTFs as similar when the differences are around the variability of the measurements.

This result suggests that small changes in the accommodation during the recording time do not reduce the quality of the retinal images, compared with that obtained when accommodation is paralyzed. In other words, the estimates of optical performance obtained with paralyzed accommodation are a good approximation of the eye's image quality under normal viewing conditions in far vision. However, it must be mentioned that non correct accommodation will largely reduce the image quality as compared with the best image with paralyzed accommodation.

MTFs for the unaccommodated and accommodated eye

Figure 5 shows the MTFs in four subjects obtained for a stimulus vergence of 0 D (unaccommodated eye; solid line) and -4 D (accommodated eye; dashed line) corresponding to conditions a) of the experimental procedure. In the particular case of subject MC, the youngest subject, we use a stimulus with a vergence of -5.5 D instead -4 D. The retinal image quality in the accommodated eye is similar to or slightly worse than in the unaccommodated one. The specific differences in the MTFs obtained for near and far vision depends on the subject. For instance, the MTF of the accommodated eye of subject AM is worse for practically all spatial frequencies

compared with the MTF for the unaccommodated eye. In the case of subject MC, both MTFs are very

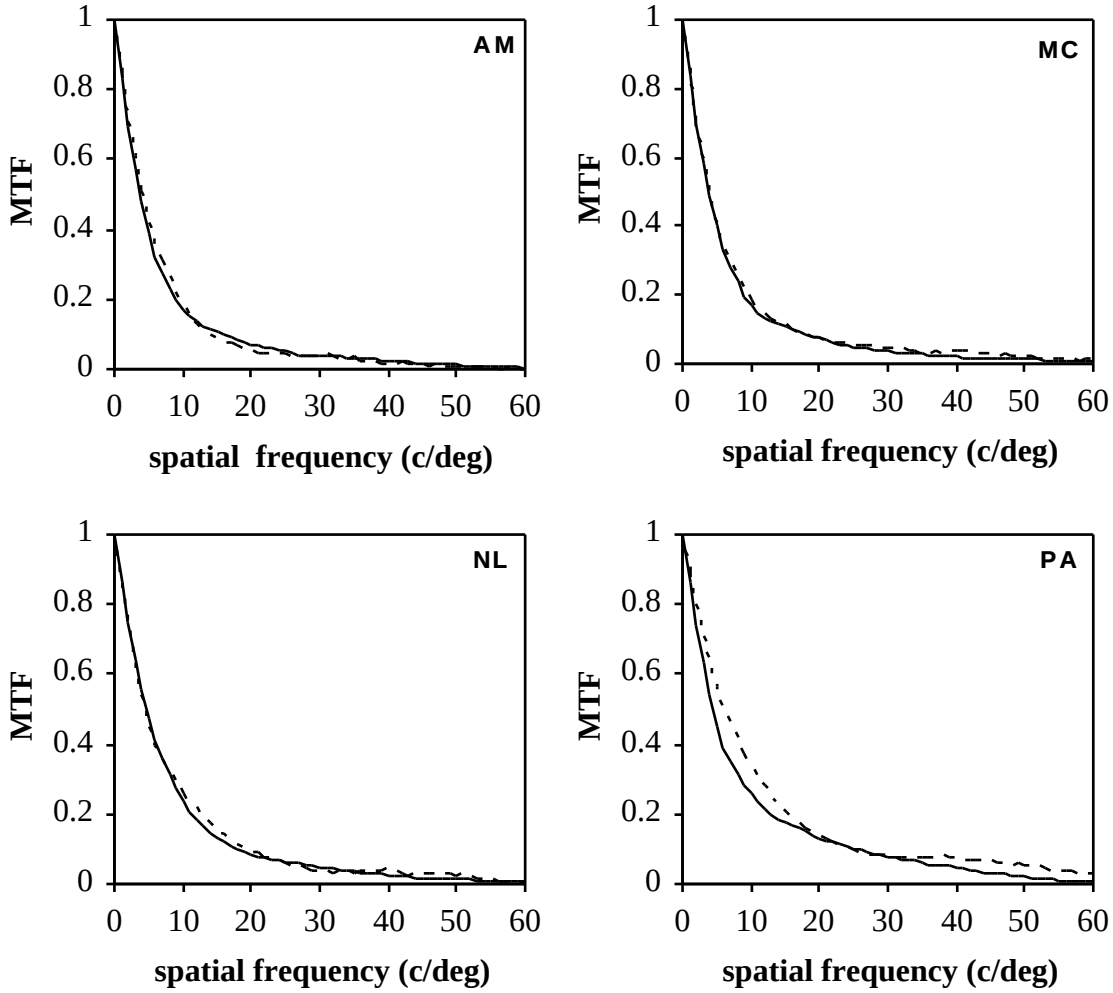

Figure 6.- MTFs (5 mm pupil diameter) in four subjects calculated when avoiding the effect of the accommodation error in near vision (dashed lines). The solid lines represent the MTF for a stimulus at infinity (the solid lines in Fig. 5).

similar, and for subject PA, the differences in the MTFs depend on the spatial frequency.

Effect of the focusing accommodative error in the MTF

By recording double-pass images under conditions b) of the experimental procedure it is possible to estimate the MTF that would correspond to the eye without accommodative error. Figure 6 shows these MTFs (dashed line) for each subject calculated using equation (8), that is, when the effect caused by the focusing error of accommodation in the second pass is avoided. These MTFs are better than those including the accommodative error in every subject and over the entire spatial frequency range (the dashed lines in figures 5 and 6 should be compared). It must be noted that the effect is small because we found very small values of accommodative error. In far vision, we found no error, except for subject MC with a value of +0.08 D. For near vision, the values of the accommodative defocus were 0.11 D for subjects AM, NL, PA and 0.08 D for MC. The MTFs calculated in the unaccommodated eye (where the error of accommodation was normally zero) and in the accommodated eye without accommodative error are very similar (see panels in figure 6).

Changes in the asymmetries of the double-pass image with accommodation

We used different pupil diameters in the first and second pass to obtain information on the asymmetries of the retinal image, both in the accommodated and unaccommodated eye (configuration c) of the experimental procedure). Figure 7 shows the contour plots of the double-pass retinal images for the unaccommodated and accommodated eye in the four subjects considered. These images are a low resolution version of the actual ocular point spread function (Artal *et al.*, 1995a). The shape of the retinal images in the

accommodated eye are substantially different from that of the unaccommodated eye and in general more radial symmetric in the accommodated eye.

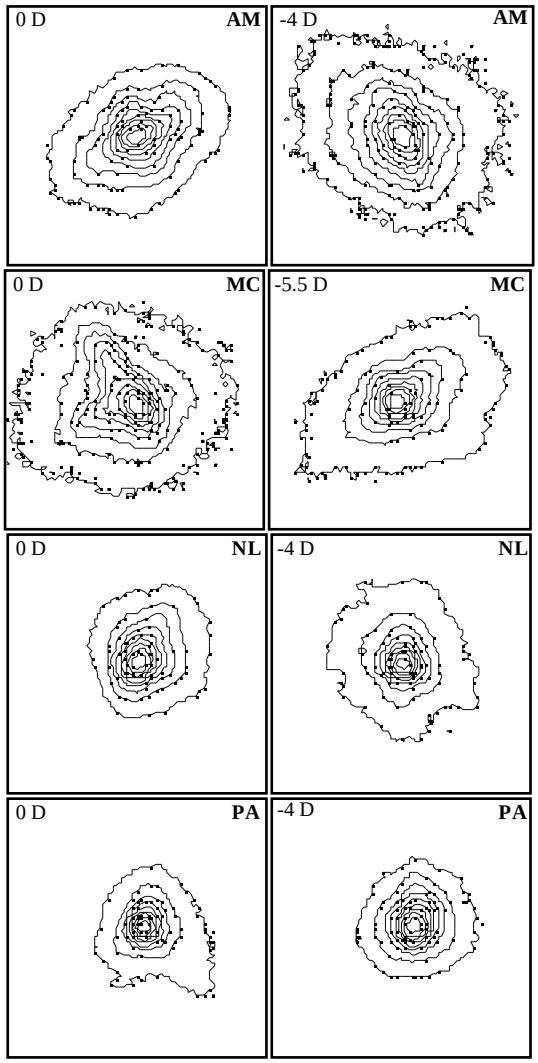

Figure 7.- Changes in asymmetries of the double pass image with accommodation in four subjects. Left and right columns represent the contour line images of the double pass images for non-accommodation and accommodation eyes respectively (see values in the left top corner of each image for specific values of the vergence of the stimulus). Each image subtends a retinal field of 14.7 minutes. Each contour line differs 10 % in the relative brightness to the very next one.

DISCUSSION

We have built a new near-infrared double-pass optometer, with two independent optical paths in both the ingoing and outgoing passes, to measure the optical performance of the eye in natural viewing with an accommodative stimulus placed at different distances. We first explored the effect of the microfluctuations, drifts and slow changes of accommodation on time-averaged measurements of retinal image quality. We recorded five-seconds exposure double-pass images, both with paralyzed and natural

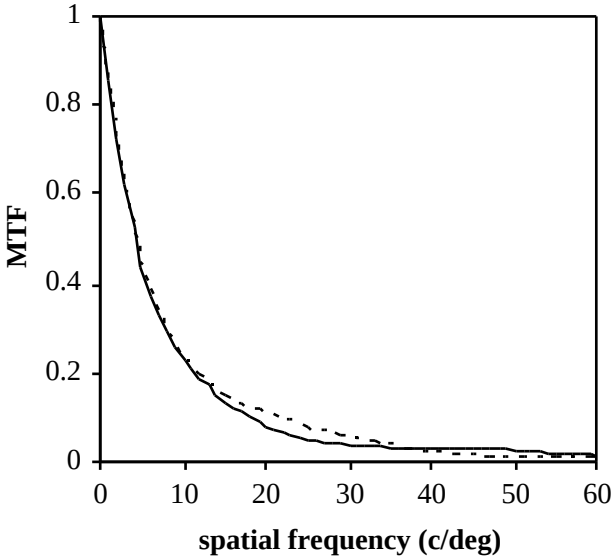

Figure 8.- Effect of the accommodative miosis in the MTF of subject NL when using a polychromatic stimulus at a vergence of 0 D with of 5.4 mm pupil (solid line) and at a vergence of -4 D for which the pupil diameter is 3.5 mm (dashed line).

accommodation, while the subject kept accommodation of the stimulus as stable as possible. The MTFs obtained under the two conditions were quite similar, showing that the overall optical performance, in terms of the radially averaged MTF, of the unaccommodated eye is similar to that of the eye under cycloplegia.

We also found similar MTFs in the unaccommodated and accommodated eye, although there is a tendency for a better MTF in the unaccommodated eye. This result agrees with previous works (Atchison *et al*., 1995) who, using others techniques, found on average, similar values of third and fourth order aberrations for the accommodated and unaccommodated eye. One of the points in which the work of Atchison *et al*., (1995) differs from ours is that they concentrated their studies on just third and fourth order wave aberrations. However, defocus due to accommodative error is responsible for a decrease in the MTF of the accommodated eye. Charman (1995) has pointed out that defocus could be the most important cause for image degradation in the accommodated eye. On that assumption, we further analyzed the actual effect that defocusing due to errors in the accommodative response have on the overall MTF. With the best refractive correction for a red stimulus, we found no significant accommodative errors for a stimulus placed at 0 D. For a stimulus with a vergence of -4 D, the typical accommodative lag was 0.11 D. These values are smaller than the subjective depth-of-focus, but it is four times the minimum

experimental error. It should be also considered that although this accommodative lag produces a slightly lower MTF for near-infrared light, the difference will become larger when rescaling the spatial frequency for visible wavelengths (López-Gil and Artal, 1997). We found that by avoiding the effect of the accommodative error, the MTF calculated for the accommodated eye is very similar to the MTF of the unaccommodated eye, where normally no accommodative error was found.

On the other hand, our daily experience shows that, in general, there is no appreciable loss in visual performance between distant and near objects viewed at the same angle. This suggests that, under normal viewing conditions, the overall image quality should be similar for both near and distant objects. Our experimental conditions did not exactly duplicate natural viewing because we used the same fixed size artificial pupil for both accommodative states we analyzed. But it is well known that during accommodation, there is a decrease in pupil diameter, accommodative miosis, that also plays a role in retinal image quality. To test the effect of pupil diameter, we also measured the MTF under completely normal viewing conditions. In this case, we measured the accommodated and unaccommodated eye of subject NL using a polychromatic stimulus (E) (the red color filter (F) was removed in the set-up). We compensated the chromatic difference in focus between the infrared source and the polychromatic stimulus (-0.72 D) and measured for 0 D stimulus vergence for a pupil diameter around 5.4 mm. The pupil diameter became 3.5 mm for a stimulus vergence of -4 D under the same experimental conditions. In the latter case, the accommodative error was -0.23 D. Figure 8 shows the MTFs under these conditions. In this case, although the accommodative error is now almost 0.25 D, the two MTFs are quite similar. However, some differences in the modulation values can be found in the middle and high spatial frequency range. This result shows that accommodative miosis and defocus error have a somehow contrary effect, resulting in an overall image performance in the accommodated eye similar to that of the unaccommodated eye. While the retinal image is slightly defocused for near targets, a reduction in pupil diameter compensates in part for the loss in image quality in the final retinal image. However, the changes in the modulation transfer with accommodation can not be explained solely in terms of these two factors. For instance, in subject PA at high frequencies, the MTF of the accommodated eye, where the accommodative error has been avoided (Fig. 6) is higher than the MTF for the unaccommodated eye.

These results suggest that ocular aberrations other than accommodative defocus are changing and modifying the retinal image quality of the accommodated eye. This is also clearly shown by the results of the change of retinal image shape with accommodation (Fig. 7). We used unequal entrance and exit pupil sizes in the double-pass apparatus to obtain information on the actual shape of the retinal PSF. The shape of the retinal image clearly changes with accommodation, and in general, the double-pass images for the accommodated eye tend to be more symmetric, although the particular changes are dependent on the subject. This result can be explained in terms of a decrease in the non-symmetric coma-like aberrations with accommodation and/or an increase of other symmetric aberrations, such as defocus, that hide the asymmetries present in the retinal image of the unaccommodated eye. A special case is subject AM, whose double-pass images showed some uncorrected astigmatism for both accommodative states. The double-pass images for this subject (Fig. 7) show that the astigmatism axis changes with accommodation. The question that remains is whether these changes in the shape of the retinal images are due either to a modification in the amount of asymmetric aberrations or to a different appearance of the point spread produced by a distinct balance of defocusing and spherical aberration. This question could be answered by further analyzing measurements of ocular aberrations with accommodation. Moreover, the same methodology presented in this work could be applied to additional studies of the aging eye or could be modified to perform real-time measurements of the relationship between accommodation and retinal image quality.

ACKNOWLEDGMENTS

This research was partially supported by grants from the Dirección General de Investigación Científica y Técnica (PB94-1138-C02-01) and Región de Murcia (COM 06/96). We thank Howard Howland, Leilani Peck, David Atchison and two anonymous reviewers for useful suggestions on the manuscript.

REFERENCES

Arnulf, A. (1965). Le système optique de l'oeil en vision photopique et mésopique. In Performance of the eye at low luminances, (pp. 135-151). Excerpta Medica International Congress Series No. 125.

Artal, P., Iglesias, I., López-Gil, N., and Green, D. G. (1995a). Double-pass measurements of the retinal-image quality with unequal entrance and exit pupil sizes and

the reversibility of the eye's optical system. J. Opt. Soc. Am. A, 12, 2358-2366.
Artal, P., Marcos, S., Navarro, R. and Williams. D. R. (1995b): Odd aberrations and double-pass measurements of retinal image quality. J. Opt. Soc. Am. A, 12 195-201.
Artal, P., and Navarro, R. (1994). Monochromatic modulation transfer function of the human eye for different pupil diameters: an analytical expression. J. Opt. Soc. Am. A, 11, 245-249.
Atchison, D. A., Collins, M. J., Wildsoet, C. F., Christensen, J., and Waterworth, M. D. (1995). Measurement of monochromatic ocular aberrations of human eyes as a function of accomodation by the Howland aberroscope technique. Vision Res., 35, 313-323.
Bartmann, M., and Schaeffel, F. (1994). A simple mechanism for emmetropization without cues from accommodation or colour. Vision Res., 34, 873-876.
Bennett, A. G., and Rabbetts, R. B. (1894). Clinical Visual Optics (2 ed.). Butterworth-Heinemann.
Berny, F., and Slansky, S. (1969). Wavefront determination resulting from Foucault Test as applied to the human eye and visual instruments. In J. H. Dickson (Eds.), (pp. 375-386). London: Oriel.
Campbell, M. C. W., Harrison, E. M., and Simonet, P. (1990). Psychophysical measurement of the blur on the retina due to optical aberrations of the eye. Vision Res., 30, 1587-1602.
Charman, W. N. (1995). Optics of the eye. Chapter 24. Vol. II in Handbook of Optics: Devices, measurements and properties. (2nd Ed.). M. Bass. MacGraw-Hill.
Charman, W. N., and Tucker, J. (1978). Accommodation and color. J. Opt. Soc. Am., 68, 459-471.
Ciuffreda, K. J. (1991). Accommodation and its anomalies. Chapter 11, Vol. I, in Vision and visual dysfunction. Ed. Cronly-Dillon. J. R.Macmillan Press.
Collins, M. J., Wildsoet, C., and Atchison, D. A. (1995). Monochromatic aberrations and myopia. Vision Res., 35, 1157-1163.
Glasser A. and Campbell M. C.W. (1998). Presbyopia and the optical changes in the human crystalline lens with age. Vision Res., 38, 209-229.
Goodman, J. W. (1996). Introduccion to Fourier Optics. (2ª ed.). McGraw-Hill.
Griffin, D. R., Hubbard, R., and Wald, G. (1947). The sensitivity of the human eye to infra-red radiation. J. Opt. Soc. Am., 37, 546-554
Howland, H. C., and Buettner, J. (1989). Computing high order wave aberration coefficients from variations of best focus for small artificial pupils. Vision Res., 29, 979-983.
Howland, H. C., and Howland, B. (1977). A subjective method for the measurement of monochromatic aberrations of the eye. J. Opt. Soc. Am., 67, 1508-1518.
Ivanoff, A. (1947). Les aberrations de chromatisme et de sphéricité de l'oeil. Revue D'Optique, 26, 145-166.
Jenkins, T. C. A. (1963). Aberrations of the eye and their effects on vision: part I. British Journal of Physiological Optics, 20, 59-91.
Kruger, P. B., S. Mathews, M. Katz, K. Aggarwala and S. Nowbotsing (1997). Accommodation without feedback suggests directional signals specify ocular focus. Vision Res., 37, 2511-2526.
Koomen, M., Tousey, R. and Scolnik, R. (1949). The spherical aberration of the eye. J. Opt. Soc. Am., 39, 987-992.
Lamb, T. D. (1995). Photoreceptor spectral sensitivities: common shape in the long-wavelength region. Vision Res., 35, 3083-3091.
Liang, J., Grimm, B., Goelz, S., and Bille, J. F. (1994). Objective measurement of wave aberrations of the human eye with the use of a Hartmann-Shack wave-front sensor. J. Opt. Soc. Am. A, 11, 1949-1957.
López-Gil, N. and Artal, P. (1997). Comparison of double-pass estimates of the retinal-image quality obtained with green and near-infrared light. J. Opt. Soc. Am. A, 14, 961-971.
Lu, C., Munger, R., and Campbell, M. C. W. (1993). Monochromatic aberrations in accommodated eyes. In Technical digest series Vol. 3, Opthalmic and Visual Optics, 160-163. Optical Society of America.
Santamaría, J., Artal, P., and Bescós, J. (1987). Determination of the point-spread function of human eyes using a hybrid optical-digital method. J. Opt. Soc. Am. A, 4, 1109-1114.
Smirnov, M. S. (1961). Measurement of the wave aberration of the human eye. Biofizika, 6, 776-795.
Thibos, L. N., Ye, M., Zhang, X., and Bradley, A. (1992). The chromatic eye: a new reduced-eye model of ocular chromatic aberration in humans. App. Opt., 31, 3594-3600.
van den Brink, G. (1962). Meaurements of the geometrical aberrations of the eye. Vision Res., 2, 233-244.
Walsh, G., Charman, W. N., and Howland, H. C. (1984). Objective technique for the determination of monochromatic aberrations of the human eye. J. Opt. Soc. Am. A, 1, 987-992.
Wildsoet, C. F., Howland, H. C., Falconer, S., and Dick, K. (1993). Chromatic aberration and accommodation: their role in emmetropization in the chick. Vision Res., 33, 1593-1603.
Williams, D. R., Artal, P., Navarro, R., McMahon, M. J. and Brainard, D. H. (1996). Off-axis optical quality and retinal sampling in the human eye. Vision Res., 36, 1103-1114.